Original Paper

Environ. Control Biol., **55** (1), 41–51, 2017
DOI: 10.2525/ecb.55.51

Blossom End Rot Tomato Fruit Diagnosis for *In Situ* Cell Analyses with Real Time Pico-Pressure Probe Ionization Mass Spectrometry

Yousef GHOLIPOUR[1], Rosa ERRA-BALSELLS[2] and Hiroshi NONAMI[1]

[1] *Plant Biophysics/Biochemistry Research Laboratory, Faculty of Agriculture, Ehime University, 3–5–7 Tarumi, Matsuyama, Ehime 790–8566, Japan*
[2] *CIHIDECAR-CONICET, Departamento de Química Orgánica, Facultad de Ciencias Exactas y Naturales, Universidad de Buenos Aires, Pabellón II, 3 P, Ciudad Universitaria, 1428-Buenos Aires, Argentina*

(Received August 29, 2016; Accepted November 15, 2016)

By combining a cell pressure probe and an Orbitrap mass spectrometer, quantitative snapshot profiles of metabolites of *in situ* plant single cells during development of blossom end rot in tomato (*Solanum lycopersicum* L.) fruit were analyzed while tomato plants were grown hydroponically in a greenhouse. By using the pressure probe, cell turgor, cell volume, cell wall elastic modulus, and hydraulic conductivity of plasma membrane were measured, followed by managed cytoplasm sampling, and osmotic and water potentials determination. It was found that the cell bursting results from alterations in water relations and cell wall properties accompanied with changes in metabolites of cells located at blossom end rot area in tomato fruit. From the water relations point of view, the loss of the elasticity and cell wall weakening, with decreased water potential and excess turgor resulted in mechanical rupture of membrane and cell wall. Abscisic acid was detected in damaged cells as a possible evidence of triggered precocious maturity. Simultaneously, a sharp rise in the concentration of phenols (coumarinate-glucoside and chlorogenic acid) and salicylic acid and decline in ascorbic acid reflected the activation of cell death process that would facilitate the deterioration of cell wall and plasma membrane.

Keywords : abscisic acid, cell turgor, elastic modulus, hydraulic conductivity, metabolomics, water relations

INTRODUCTION

Blossom end rot (BER) of tomato fruit has been identified as a physiological disorder caused by calcium (Ca) deficiency (Lyon et al., 1942). Ca has been believed to adjust the structure and properties, particularly gelation, of cell wall pectin (Jarvis, 1984). Gelation, which directly influences the elasticity and expansion of cell wall, is critically dependent on the availability of Ca in the apoplast. It has been speculated that the insufficient availability of Ca in the apoplast of expanding cells results in cell wall weakening, impairment of cell expansion, and finally cell burst and death (Ho and White, 2005). However, high Ca concentration could induce BER in tomato fruit (Nonami et al., 1995; Hossain and Nonami, 2012). Ca concentration in BER fruit was higher than that in healthy fruit (Nonami et al., 1995). Thus, it may be possible to speculate that some factors other than Ca deficiency causes BER in tomato fruit. When Ca salts were added excessively to the hydroponic solution, we could induce BER in 30–50% of fruit formed in tomato plants (Nonami et al., 1995; Hossain and Nonami, 2012). It is noteworthy that 50–70% of fruit in the same tomato plant did not exhibit BER although the fruit was exposed to the same stress condition. All cells in both BER and non-BER exhibiting fruit in the same plant had the same DNA, having different metabolisms. How was this difference induced?

Analysis of cell physical and chemical properties with single cell resolution can clarify cell to cell variations and many primary growth, disorder, or stress related phenomena that cannot be detected or fully explored through tissue-level studies. Integrative analyses of water relations and metabolomics of plant cells, therefore, can provide remarkable insights to many physiological events during growth or environmental stresses. However common water status measurements are not provided with molecular information and on other hand, a big challenge is to perform quantitative metabolite profiling at cell level. In order to investigate these distinct aspects concurrently at real time and with single cell resolution, we devised a new technique by combining a cell pressure probe (PP) and an Orbitrap mass spectrometer, named as pico-pressure probe ionization mass spectrometry (picoPPI-MS).

The PP is routinely used to analyze several properties of plant single cells including *in situ* cell volume determination (Malone and Tomos, 1990), and turgor pressure, osmotic potential, water potential, plasma membrane hydraulic conductivity, and cell wall elastic modulus measurements (Nonami and Boyer, 1989; Nonami and Schulze, 1989; Boyer, 1995). In addition PP uniquely facilitated managed picoliter sampling of *in situ* single cell solution, since sample volume can be controlled and measured (Nonami and Schulze, 1989). In picoPPI-MS, after the

Corresponding author : Hiroshi Nonami, fax: +81–89–946–9824,
e-mail : nonami@agr.ehime-u.ac.jp

water status measurements and cell sampling, the profiling and quantitation of metabolites in the cell sample are performed by applying high voltage to the tip of PP quartz capillary and sample solution inside. Consequently, metabolites were directly nebulized/ionized and enter into the mass spectrometer.

We investigated changes in water relations and metabolite content leading to cell bursting in single cells located in BER area in tomato fruits. BER is a common but poorly understood disorder in tomato production that appears early in fruit growth with visible symptoms of the deterioration and necrosis of pericarp tissue. Unlike programmed plant cell death which is an active and normal process during life (Cohen, 1993; Pennell and Lamb, 1997), stresses or physiological disorders result in cell necrosis, which is speculated to be an irreversible, passive, and non-physiological process involving cell swelling, membrane rupture and cell bursting (Cohen, 1993; Pennell and Lamb, 1997; Laporte et al., 2007). However, it would expect cell bursting to be the result of an extensive physiological disorder originated from changes in turgor and osmotic potentials, cell wall and plasma membrane, and metabolism. On the other hand, tissue level analyses cannot facilitate exploring and understanding the cell bursting mechanisms. The picoPPI-MS technique could reveal changes in water relations and metabolites in an integrative and complementary way so that mechanisms led to bursting and necrotic death of BER affected cells could be explained.

MATERIALS AND METHODS

Plant materials

Tomato plants were cultivated as shown in the previous work (Hossain and Nonami, 2011; 2012). Tomato seeds (*Solanum lycopersicum* L. cv. Momotaro) (Takii & Co., Ltd., Kyoto, Japan) were germinated in the laboratory at 25±1°C in the dark in February 2010. Two-week-old seedlings were grown hydroponically in plastic planter using Otsukahouse nutrient solution No. 1 & 2 (Otsuka Chemical Co., Ltd., Osaka, Japan). At 4-5 true leaves stage, healthy and uniform seedlings were transplanted in 15 L size plastic pot containing nutrient solution (EC 1.0 mS cm^{-1}, pH 6.25) in the greenhouse. Nutrient solution in pots was replaced once a week with adjusted EC and pH. The concentration of nutrient solution was increased from 1.0 to 1.2 mS cm^{-1} during first flowering to third flowering time. After third flowering to fruit harvest, the electrical conductivity of nutrient solution was adjusted 1.5 mS cm^{-1}. Excess calcium ($CaCl_2 \cdot 2H_2O$) was added into above nutrient solution and elevated solution electrical conductivity (EC) 8 mS cm^{-1} which provided additional 32.3 mM Ca L^{-1} into regular nutrient solution to induce BER in fruit. Before application of treatment, all plants were grown with the same concentration of solution (EC 1.0 mS cm^{-1}) then solution with EC 8 mS cm^{-1} was applied when flowers fully bloomed in the first truss. At the same time EC 1.5 mS cm^{-1} was used for control plants. Flowers were artificially pollinated by using hormone (Tomatotone, Ishihara Bioscience Co., Tokyo, Japan) and day after flowering was considered from the date of hormone application. Hydroponically grown 3-week-old tomato fruits with apparent BER symptoms were picked up and immediately put into a Styrofoam box and their fruit peduncles were kept in water. Healthy fruit which did not exhibit BER in the same plant was used as the control. A greenhouse had heating systems to keep the temperature over the minimum of 15°C throughout the year. BER is more frequent in early spring in the greenhouse when the maximum temperature reaches 30°C. With the rise of the minimum temperature over 15°C in the following months the occurrence of BER decreases. During measurement experiments fruit peduncles were continuously kept in distilled water and fruits were covered with a sheet of plastic film but exposing a small area for measurements. The temperature of measurement room was adjusted to 25°C.

Cell pressure probe measurements

The pico-pressure probe ionization mass spectrometry (picoPPI-MS) setup is well described in the work of Gholipour et al. (2013). The setup was similar as follows: The PP instrument and plant stand were placed on a magnetically-floated vibration-free table (Magfloat™, Sanaikogyo Co., Ltd., Japan). A quartz capillary with submicrometer open tip was air-tightly connected to a pressure sensor (Kulite Semiconductor Products, Inc., model XTM-190M-7-BAR-VG, NJ, USA) through a tube filled with silicon oil (Wacker Silicone AS 4, Wacker-chemie GmbH, München, Germany). A quartz capillary micropipette was filled with a mixture (5:1, v/v) of silicon oil and an engine oil supplement (MolySpeed® 21, Sumico Co., Japan). Analyses were carried out on cells located in 1 cm^2 of outer pericarp tissue around BER area under cuticle and down to the depth of about 600 μm from the surface.

In situ cell turgor, cell wall elasticity, and membrane permeability measurements were conducted as described before (Hüsken et al., 1978; Nonami and Boyer, 1989; 1993; Boyer, 1995). The capillary was penetrated into a living cell and a part of cell solution, about 200 pL in case of expanding parenchyma cells in tomato fruit pericarp, was pushed into the capillary due to turgor pressure created by extended plasma membrane and cell wall complex.

PP is used to measure cell water potential, a fundamental concept in plant biology (Nonami and Schulze, 1989). A part of cell solution sample is loaded onto a cryo-osmometer plate to measure osmotic potential (Shackel, 1987; Nonami and Schulze, 1989) as shown in a photo in Gholipour et al. (2012). Water potential of the cell is then obtained by summing up value of turgor and that of osmotic potential. By summing the turgor pressure (Ψ_P) and osmotic potential (Ψ_S) values, water potential (Ψ_W) of the cell is calculated ($\Psi_W = \Psi_P + \Psi_S$). PP can be also used for cell volume measurement after turgor measurement (Malone and Tomos, 1990; Gholipour et al., 2012). Capillary movement and penetration depth were monitored and measured carefully by a piezo manipulator (PM101, Märzhäuser Wetzlar, Germany) and corresponding cells were identified under microscope for volume measurement (Gholipour et al., 2012).

Mass spectrometry analyses

After cell water relations analyses followed by managed cell sampling, the PP was flipped around horizontally so that the quartz capillary tip was located close to the entrance (cone orifice) of a mass spectrometer (Gholipour et al., 2013). An atmospheric pressure ionization method (Fenn et al., 1989; Cooks et al., 2006) based on the electrification of the picosample at the tip of the PP quartz capillary was developed (Gholipour et al., 2013). The built-in ion source of an Exactive Orbitrap™ mass spectrometer (Thermo Fisher Scientific K.K., Yokohama, Japan) was substituted by the quartz capillary connected to the PP. To maximize the sensitivity, automatic gain control (ion injection to mass analyzer) was set to high dynamic range, time of injection of ion package to 250 milliseconds, and the temperature of sampling tube of mass spectrometer to 200°C. By applying high voltage (Matsusada Precision Inc. and ARIOS Inc., Japan) to the tip, analyte solution was directly nebulized/ionized into the mass spectrometer (Gholipour et al., 2013). By using an aqueous KCl solution as blank, mass spectra of cell samples were background-subtracted with using Thermo™ Xcalibur™ (Thermo Fisher Scientific K.K., Yokohama, Japan) and metabolites were characterized in both positive and negative ion modes.

For quantitation experiments, 100 and 600 picoliter volumes of 0.1–25 mM aqueous standard solutions (glucose, sucrose, malic acid, nicotinic acid, abscisic acid, salicylic acid, hydroxyproline, ascorbic acid, gluconic acid and citric acid; Wako Chemicals, Japan) were loaded in a PP capillary tip. Signal intensity vs. concentration of the standard in the stock solution (Supplemental data shown in Gholipour et al., 2013) and vs. numbers of moles of the standard compounds in the picosample injected (Supplemental data shown in Gholipour et al., 2013) were used for linearity examination. Depending on the standard, these measurements were performed in the positive and/or negative ion mode for proper quantification. PicoPPI-MS of cell samples for qualitative and quantitative analyses were also carried out in both positive and negative ion modes as shown by Gholipour et al. (2013).

RESULTS

The technique

The analysis principally included three steps of probing, sampling and profiling. Unlike other cell sampling methods based on the penetration of simple glass capillary tip (Tejedor et al., 2009) or of a metal needle (as in probe-electrospray, Yu et al., 2009), use of a cell PP provided fully manageable probing and picoliter sampling that included confirmation of capillary localization, the absence of leakage (hydraulic continuity test), and cell sample volume measurement (Gholipour et al., 2012). The cell type and location can be distinguished by turgor pressure probing (Gholipour et al., 2012). By recording depth of penetration and with anatomy information in hand, the cell layer in which capillary is located can be determined with a position indicator of a piezomotor manipulator system (Gholipour et al., 2012). In addition, it is uniquely possible to access and sample a deeper cell with minimum contaminations of shallower cell solution (Gholipour et al., 2012).

Sample preparation, pretreatment and preprocessing are not required in picoPPI-MS. Cell solution can be analyzed directly by using the Orbitrap MS as high-resolution mass spectrometry. In picoPPI-MS there is no flow of the analyte solution and indeed the sample is ionized and introduced into the mass spectrometer without the addition of a stream solvent or auxiliary gas spray (Gholipour et al., 2013). Since the PP instrument was located close to a mass spectrometer, metabolites were ionized/detected immediately after *in situ* cell water status measurements and sampling, with negligible sample loss or evaporation. Because of very high molecular mass resolution, a wide range of detection and a very low limit of detection, many metabolites from sugars and amino acids to organic acids and phytohormones were detected in both positive and negative ion modes (Table 1). More than 50 molecules were identified in a single cell of tomato fruit simultaneously as shown in Table 1. The number of metabolites detected in the positive ion mode was higher than that in the negative mode. Nevertheless, less background noise signals appeared in the negative mode.

By loading 100 and 600 pL volumes and different concentrations of standard solutions, the dependence of signal intensity on concentration was determined as shown in Supplemental data of Gholipour et al. (2013). Additionally, abscisic acid, hydroxylproline, nicotinic acid gluconic acid and salicylic acid were used to make the standard curve for quantification (data are now shown). Good linearity showed the applicability of picoPPI-MS for quantitative metabolite profiling of sub-picoliter samples containing a mixture of metabolites with a wide range of concentrations. By collecting results of different measurements into single standard graphs for each metabolites quantitation was successfully carried out. The ranges of volume and concentration were corresponding to the cell solution volume (about 200 pL in average) and concentrations of examined metabolites in tomato fruit cells. Table 2 shows the average concentration of metabolites, measured with picoPPI-MS, in the solution of expanding parenchyma cells of a healthy 3-week-old fruit. By using such standard curves, metabolite concentrations in normal or dissolving or damaged cells located at blossom end rot (BER) affected area (Fig. 1b) of 3-week-old fruit are shown in Table 3.

Analysis of BER

Developmental time sequence of tomato fruit used in the present study is shown in Fig. 1a. BER appeared in a 3-week-old fruit as shown in Fig. 1b and cell rupture and cell leakage could be observed among damaged cells denoted “C” zone under a microscope. The size of parenchyma cells located in distal blossom end area of fruit pericarp, and that of cells located about 1 cm farther are shown in Fig. 1c. Cells in BER-affected fruits failed to expand normally, and consequently were smaller than those in healthy fruit having the similar age and size (Fig. 1c). Anatomy of the apparently damaged area revealed the

Table 1 Metabolites detected in cell picosamples from a healthy tomato fruit in positive ($[M+H]^+$, $[M+Na]^+$, and/or $[M+K]^+$), and negative modes ($[M-H]^-$).

Detected mass	interpretation & exact mass						
		+H	+K	+Na	−H	Δm (Da)	*Ref.*
89.1112	putrescine	89.1073				0.0039	*1,2,3*
102.0957	acetoacetic acic	102.0910				0.0047	*2*
104.0335	serine				104.0342	−0.0007	*1,2*
112.0910	oxo-pentadienoic acid	112.0850				0.0060	*2*
116.0065	valine				116.0705	−0.0005	*1,2*
126.0520	GABA			126.0524		−0.0006	*1*
130.0550	5-oxoproline	130.0498				0.0052	*1,2*
131.0151	glycerol		131.0105			0.0046	*1,2*
131.0441	asparagine				131.0451	−0.0010	*1,2*
132.0287	aspartic acid				132.0292	−0.0005	*1,2,4*
132.1011	leucine/Isoleucine	132.1019				−0.0008	*1,2*
133.0131	malic acid				133.0132	−0.0001	*1,2,4*
133.0663	asparagine	133.0607				0.0056	*1,2*
135.0260	malic acid	135.0288				−0.0028	*1,2*
137.0191	salicylic acid				137.0233	0.0042	*2*
138.0520	proline			138.05244		−0.0004	*1,2*
138.0950	tyramine	138.0916				0.0034	*1,2*
140.0516	acetoacetic acid		140.0460			0.0056	*2*
142.0309	GABA		142.0265			0.0044	*1*
145.0601	glutamine				145.0608	−0.0007	*1,2*
146.0448	glutamic acid				146.0449	−0.0001	*1,2,4*
146.0227	nicotinic acid			146.0214		0.0013	*1,2*
146.1693	aminoadiapatesemialdehyde	146.1690				0.0003	*1,2*
147.0772	glutamine	147.0764				0.0008	*2*
148.0636	glutamic acid	148.0605				0.0031	*1,2*
154.0258	proline		154.0263			−0.0005	*1,2*
156.0460	valine		156.0421			0.0039	*1,2*
158.0255	threonine		158.0214			0.0041	*1,2*
165.0723	thymine		165.0790			−0.0067	*2*
166.0850	phenylalanine	166.0858				−0.0008	*1,2*
169.0956	lysine			169.0950		0.0006	*1,2*
170.0586	leucine		170.0578			0.0008	*1,2*
171.0213	asparagine		171.0166			0.0047	*1,2*
172.0065	aspartic acid		172.0007			0.0058	*1,2*
173.0078	dehydroascorbic acid				173.0080	−0.0002	*1,2*
175.0233	ascorbic acid				175.0237	−0.0004	*1,2,4*
175.1149	arginine	175.1189				−0.0040	*1,2*
177.0370	ascorbic acid	177.0393				−0.0023	*1,2*
179.0553	hexose (mainly glucose)				179.0550	0.0003	*1,2*
181.0680	hexose(mainly glucose)	181.0706				−0.0026	*1,2*
185.0373	glutamine		185.0323			0.0050	*1,2*
191.0176	citric/isocitric acid				191.0186	−0.0010	*1,2,4*
192.0229	carboxyphosphonoenolpyruvic				192.0210	0.0019	*2*
193.0678	quinic acid	193.0706				−0.0028	*1,2*
195.0506	gluconic acid				195.0499	0.0007	*1,2,4*
197.0632	gluconic acid	197.0655				−0.0023	*1,2*
199.0784	erythrose phosphate	199.0770				0.0014	*2*
219.0237	hexose		219.0265			−0.0028	*1,2*
230.9971	citric/isocitric acid		230.9901			0.0070	*1,2*
234.1414	hydroxymethyldihydropterin		234.1440			−0.0026	*2*
243.0255	tryptophan			243.0259		−0.0004	*1,2*
259.0215	hexose-6-phosphate				259.0213	0.0002	*1,2,3*
262.0374	hexose-6-phosphate	262.0369				0.0005	*1,2,3*
283.0183	hexose-6-phosphate			283.0189		−0.0006	*1,2,3*
297.0899	hexose-6-phosphate		297.0850			0.0049	*2*
303.0721	abscisic acid		303.0790			−0.0069	*2*
326.1090	coumarinate-glucoside	326.0996				0.0094	*2,5*
346.0460	glutathione		346.0469			−0.0009	*1,2*
355.1010	chlorogenic acid	355.1020				−0.0010	*1,2*
365.1177	disaccharide (sucrose)			365.1053		0.0124	*1,2*
381.0910	disaccharide (sucrose)		381.0792			0.0118	*1,2*
393.0545	chlorogenic acid		393.0579			0.034	*1,2*

[1] (Schauer, et al., 2004); [2] (http://solcyc.solgenomics.net, 2009); [3] (Carrari, et al., 2006); [4] (Gómez-Romero, et al., 2010); [5] (Moco, et al., 2006)

Table 2 The average concentration of metabolites, measured with picoPPI-MS, in the solution of expanding parenchyma cells of a healthy 3-week-old fruit.

metabolite	pmol in 200 pL of cell solution	Concentration in cell solution (mM)
Glucose (hexose)	26.01	130.07
citric acid	2.4	12.00
malic acid	0.37	1.87
Sucrose (disaccharide)	2.0	10.0
ascorbic acid	0.15	0.77
hydroxyproline	0.04	0.20
salicylic acid	0.02	0.10
nicotinic acid	0.01	0.05
gluconic acid	0.01	0.05
abscisic acid	0.008	0.04

rupture and leakage, followed by tissue breakdown and necrosis (Fig. 1b). Cells located at blossom end were smaller in BER fruits (Fig. 1c), elucidating the impairment of cell expansion of young growing parenchyma cells.

Integrative cell probing and picoPPI-MS analyses of the affected cells revealed physiological deterioration, along with physical bursting mechanisms (Table 3). A threefold increase in turgor was observed in close-to-busting cells (Table 3). Cell wall elastic modulus of those cells decreased initially and then increased in conjunction with the stress imposed by increasing turgor pressure (Table 3), indicating the cell wall was under extreme pressure in close-to-bursting cells.

Intracellular accumulation of some of metabolites including organic acids and disaccharides resulted in a decrease in osmotic potential, and thus, more negative water potential (Table 3). Consequently, more water uptake and excess turgor were induced. Lower hydraulic conductivity of plasma membrane confirmed the loss of membrane integrity in affected cells (Table 3). During normal maturity of tomato fruit, the concentration of sugars increases while the content of organic acids (mainly citric and malic acid) decreases (Ho and White, 2005). The healthy fruit in Table 2 confirmed the observation made by Ho and White (2005). In the healthy fruit, glucose (hexose) and sucrose (disaccharide) concentrations were much higher than in normal cells of fruit exhibiting BER (Tables 2 and 3). Concentrations of malic acid and ascorbic acid in the normal cells of BER fruit (Table 3) were higher than those of cells in the healthy fruit (Table 2). Thus, osmotic adjustment occurred by accumulating sugars while reducing concentrations of organic acids in the healthy fruit at low water potentials. In similar sizes of fruit shown in Fig. 1C in the same plant, the normal cells of BER fruit had lower concentrations in sugars and higher concentrations in organic acids than the healthy fruit (Tables 2 and 3). However, concentrations of citric acid, nicotinic acid and gluconic acid were similar in both normal cells of BER fruit and the healthy fruit cells (Tables 2 and 3).

The polarity switching of the Orbitrap MS can be adjusted to one full cycle in $<$ 1 sec (one full scan positive mode and one full scan negative mode at resolution setting of 10000) (Thermo Fisher Scientific Exactive™ Operating Manual). This means that molecular ions can be measured in both positive and the negative modes almost simultaneously. Figures 2 and 5–8 are shown in the positive mode and Figs. 3, 4 are shown in the negative mode. The y-axis of the figures indicates the absolute intensity which is the MS detector outputs and almost correlated to the concentrations of detected molecular ions. We observed lower hexose in close-to-burst cells than that in healthy cells at BER area in Fig. 2. Other molecular ions cannot be seen in Fig. 2 because the absolute intensity of sugar signals were too strong compared with other molecular ions. Higher organic acid concentrations (Figs. 3 and 4) were observed in affected cells. These observations are in consistent with PP measurement results elucidating impairment of membrane hydraulic conductivity in damaged cells (Table 3). It has been previously proposed that the changes in organic acids originate from malfunction of membrane channels (Chen et al., 2001), and of hexose from decreased import (Chen et al., 2001; Saure, 2001), all related to the disintegration of plasma membrane. The loss of the elasticity and weakening of cell wall, with increased water uptake and excess turgor finally led to the cell bursting due to the inability of cell to manage extreme turgor.

Additionally, in BER affecting cells, several metabolites belonging to cell responses to biotic or abiotic stresses were detected and changes in their intracellular concentration analyzed (Table 3). Increased concentration of nicotinic acid (Fig. 5) and gluconic acid (Fig. 6) observed in damaged cells is consistent with previous research which concluded their increased biosynthesis during BER (Ho and White, 2005). Abscisic acid with *de novo* synthesis (Fig. 7), increased concentration of phenols (coumarinate-glucoside, Fig. 7; and chlorogenic acid, Fig. 8), four times rise of salicylic acid (Fig. 3), and significant reduction of ascorbic acid (Fig. 4) were also observed. On the other hand, increased intracellular concentration of those metabolites contributed the reduction in osmotic potential previously mentioned (Table 3).

DISCUSSION

When salts are added to hydroponic solution, water stress is induced by osmotic stress. Proper amount of water stress will improve quality of fruit due to sugar accumulation by osmotic adjustment. A healthy 3-week-old fruit accumulated sugars while concentrations of organic acids (malic acid and ascorbic acid) became lower than the healthy cells of BER fruit at low water potential even thought they were growing in the same plant (Fig. 1, Tables 2 and 3). Salicylic acid is known to interact with ABA for osmotic adjustment on the early response of tomato plants to drought (Munoz-Espinoza et al., 2015). The healthy fruit had both salicylic and ABA with significant sugar accumulation in cells (Table 2), suggesting that osmotic adjustment was properly taking place under salt stress. Even under the same salt stress condition in the same plant, ABA was undetected and much lower concentration of salicylic acid was observed in normal cells of BER fruit with lower concentrations of sugars (Table 3). When cells became

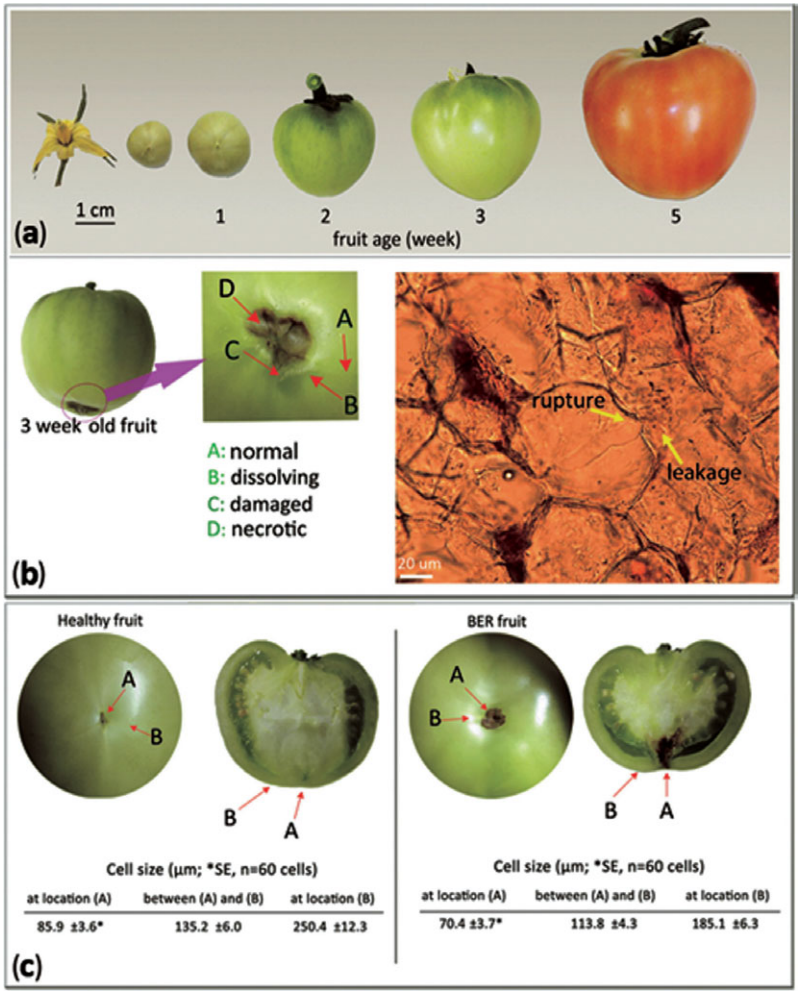

Fig. 1 Developmental time sequence of tomato fruit (a), cell location in blossom end rot (BER) affected area (A: normal, B: dissolved, C: damaged, D: necrotic) and cell photos of damaged area "C" which shows cell rupture and cell leakage (b), comparisons of cell size between healthy fruit and BER fruit (c). Cell length was measured in 60 cells and the average ±SE (standard error) is shown in (c).

Table 3 Result obtained by PP (for water relations) and PicoPPI-MS (for metabolites) of cells located at BER area of tomato fruits.

	Cells in BER area[z]		
	normal	dissolving	damaged (close-to-bursting)
Water relations (±SE, $n=8$)			
turgor pressure (Ψ_P, MPa)	+0.12±0.02	+0.22±0.09	+0.34±0.02
osmotic potential (Ψ_S, MPa)	−0.98±0.01	−1.00±0.01	−1.36±0.02
water potential (Ψ_W, MPa)	−0.86±0.02	−0.80±0.02	−1.02±0.04
cell wall elastic modulus (ε, MPa)	3.8±0.3	2.7±0.3	4.6±0.7
membrane hydraulic conductivity (L_P, m. s^{-1}. MPa^{-1})	2.1×10^{-6} ±5.5×10^{-7}	1.3×10^{-6} ±4.4×10^{-7}	1.0×10^{-6} ±2.2×10^{-7}
Metabolites (±SE, $n=5$, mM)			
citric acid	12.0±2.2	17.5±4.3	25.0±3.5
malic acid	13.9±2.1	14.1±5.4	25.0±4.7
gluconic acid	0.04±0.01	0.06±0.01	0.07±0.02
nicotinic acid	0.05±0.01	0.06±0.01	0.10±0.03
abscisic acid	not detected	not detected	0.04±0.02
salicylic acid	0.06±0.01	0.10±0.05	0.25±0.13
ascorbic acid	8.01±3.38	7.60±2.2	1.30±0.86
chlorogenic acid	0.32±0.29	0.36±0.25	1.03±0.54
coumarinate-glucoside	0.10±0.008	0.10±0.002	0.20±0.01
hexose	84.3±17.29	83.4±16.4	43.3±1.56
disaccharide	5.04±2.10	14.0±1.10	23.0±3.04
hydroxyproline	0.11±0.02	0.21±0.01	0.4±0.18

[z] photos of normal, dissolving and damaged cells are shown in Fig. 1b.

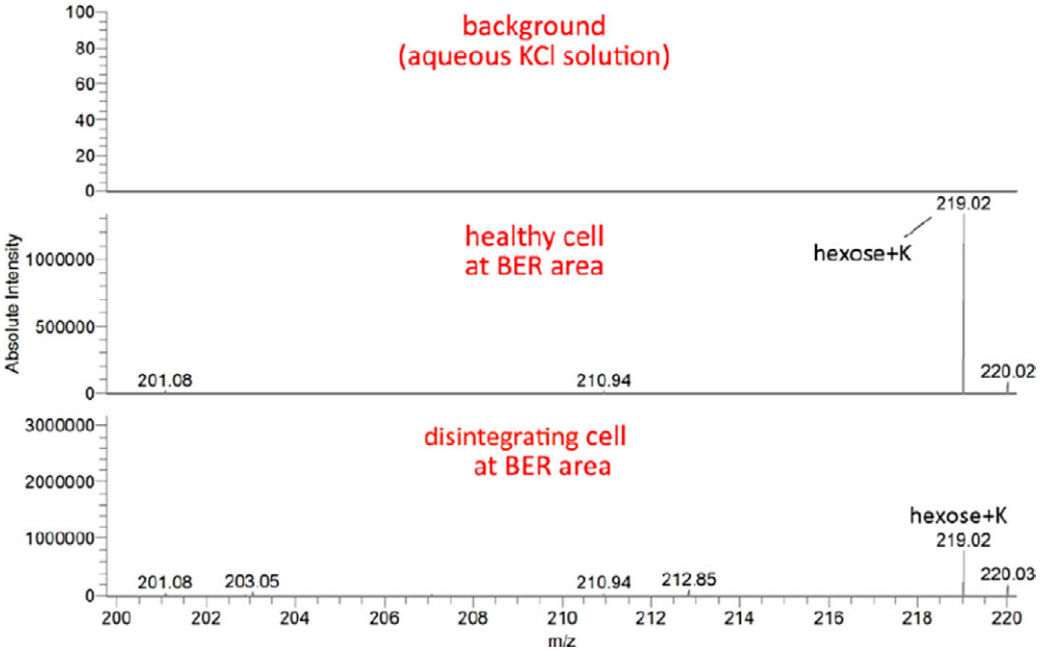

Fig. 2 PicoPPI mass spectra acquired by analyzing standard and cell solutions in positive ion mode; m/z 200–220. m/z indicates mass-to-charge ratio.

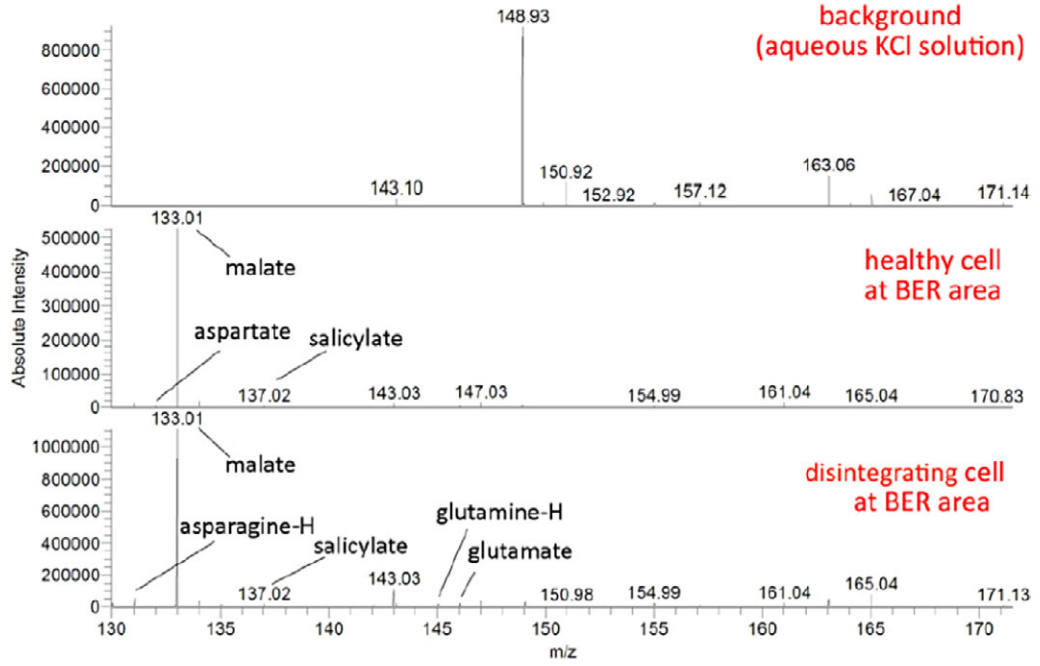

Fig. 3 PicoPPI mass spectra acquired by analyzing standard and cell solutions in negative ion mode; m/z 130–170.

close to burst, concentrations of ABA, salicylic acid, malic acid and citric acid increased significantly (Table 3). Nicotinic acid is also known to osmotic adjustment and salt tolerance (Rajasekaran et al., 2000). The concentration of nicotinic acid (Nicotinic+Na in Fig. 5) increased in close-to-bursting cells of BER fruit (Table 3). Simultaneously, concentrations of disaccharide and organic acids became higher, and turgor became larger in close-to-bursting cells (Table 3). Even though locations of the normal cell, dissolving cells and close-to-burst cells in the same BER fruit were very adjacent each other, it was found that mechanisms of osmotic adjustment and metabolisms are very different. If the analysis were conducted in the tissue level, it would not be found such phenomena. Only single cell picoPPI-MS analysis could found adjacent cell-to-cell metabolic differences in BER area.

Cell division in tomato fruit is over one week after flowering (Hossain and Nonami, 2011). BER in tomato fruit occurs commonly during cell expansion at the tip of fruit while fruit is growing rapidly in size. The normal process of cell expansion in young fruits involves cell wall relaxation followed by maintaining turgor pressure, and *de*

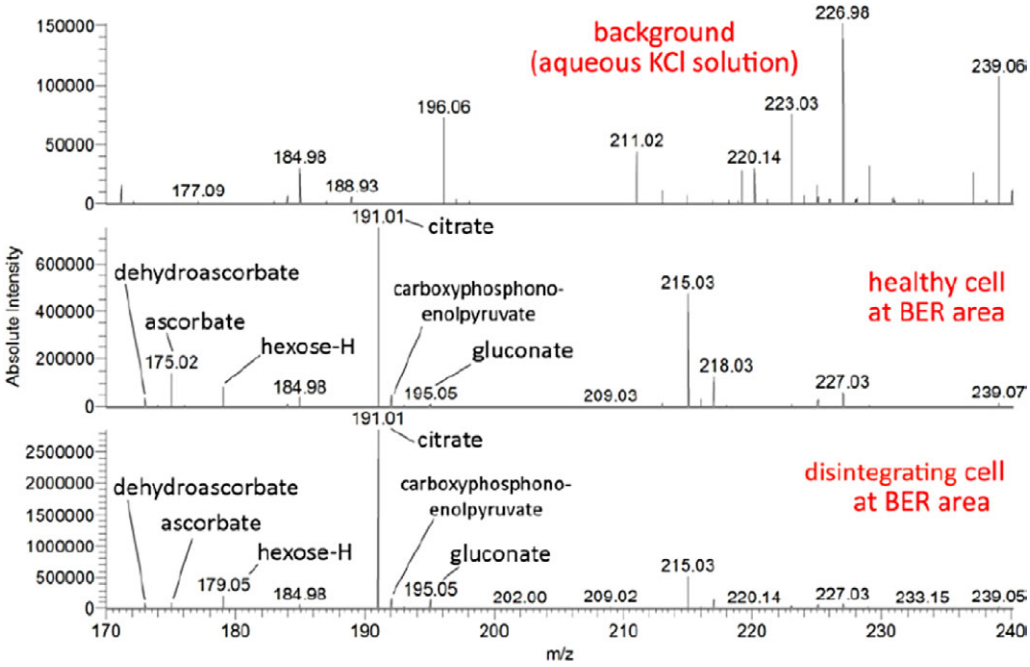

Fig. 4 PicoPPI mass spectra acquired by analyzing standard and cell solutions in negative ion mode; m/z 170–240.

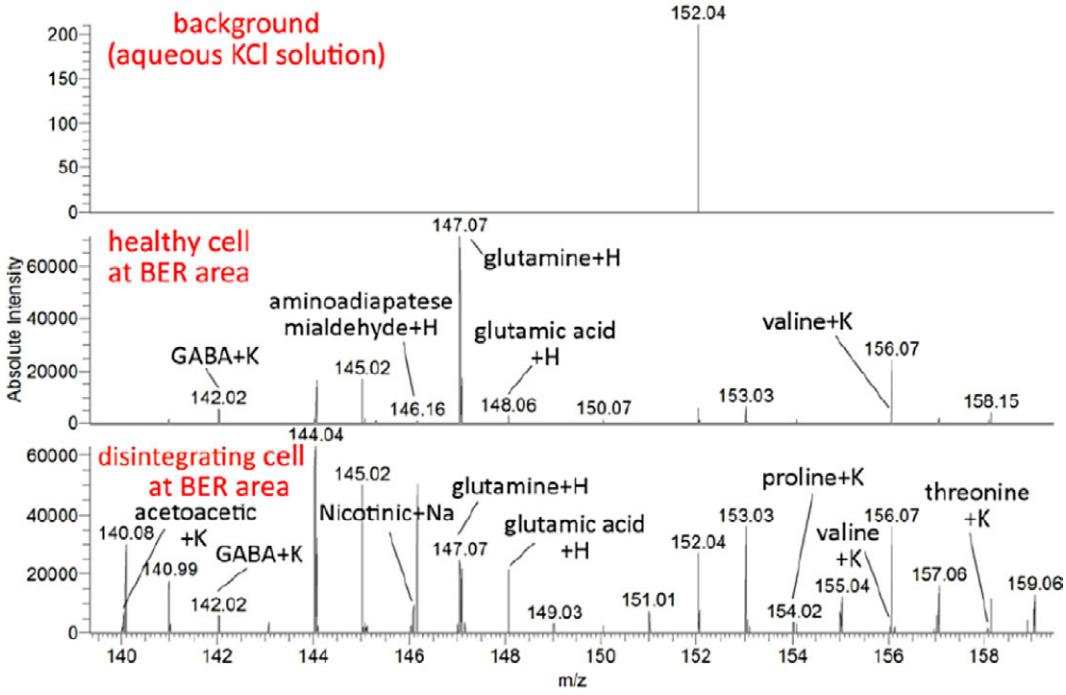

Fig. 5 PicoPPI mass spectra acquired by analyzing standard and cell solutions in positive ion mode; m/z 140–160.

novo wall synthesis to keep cell wall thickness (Taiz and Zeiger, 2006). Protoplasm expansion is driven by osmotic change and increased water uptake. In BER cell bursting resulted from excess hydrostatic pressure created by expanding protoplasm, accompanied by a weakened cell wall that is unable to elastically expand and withstand pressure. PP measurements confirmed cell wall weakening, plasma membrane impairment, and abnormal expansion. These abnormalities were reflected as the smaller size of parenchyma cells in damaged fruit pericarp (Fig. 1).

In Fig. 7, coumarinate-glucoside was found in healthy cells of BER fruit, and its concentration decreased in disintegrating cells at BER area. A coumarin derivative, morlin, was found to be an inhibitor of cortical microtubule dynamics and cellulose movement in *Arabidopsis* (DeBolt et al., 2007). Additionally, coumarins are known to be related to metabolisms in cell wall polymer lignin (Barros et al., 2016). In disintegrating cells of BER, concentration of chlorogenic acid (Fig. 8) increased, and chlorogenic acid is known to be associated with weaker structural membrane damage (Yildiz-Aktas et al., 2009). Furthermore, concentrations of gluconate (Fig. 4) and gluconic acid (Fig. 6)

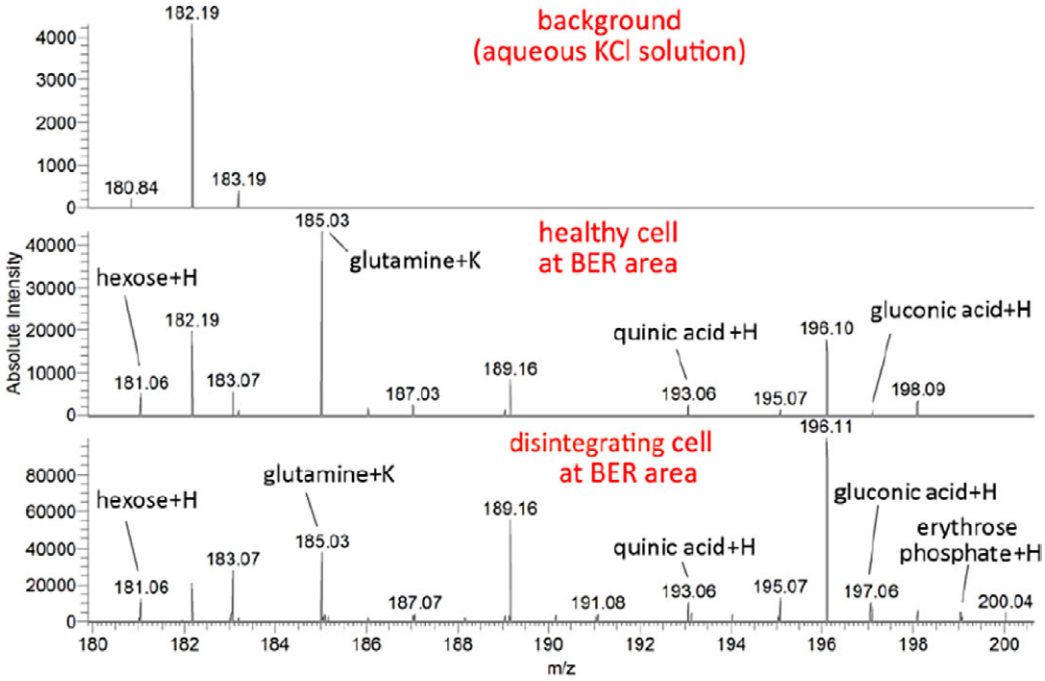

Fig. 6 PicoPPI mass spectra acquired by analyzing standard and cell solutions in positive ion mode; m/z 180–200.

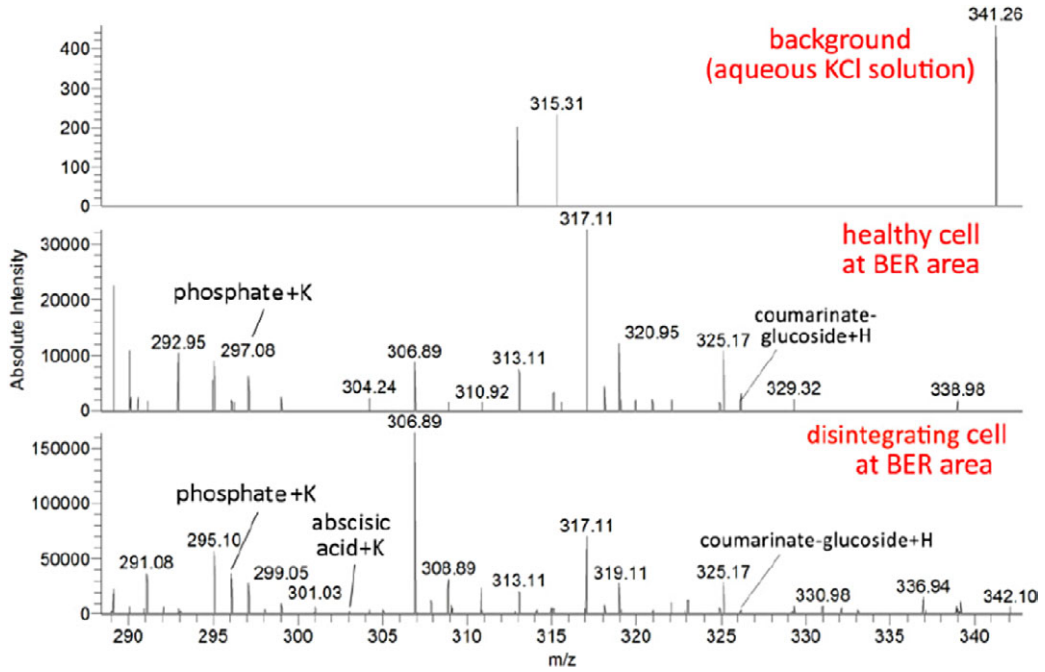

Fig. 7 PicoPPI mass spectra acquired by analyzing standard and cell solutions in positive ion mode; m/z 290–340.

increased in disintegrating cells at BER area, and those compounds are known to be strongly correlated to maturation of tomato fruit (Oms-Oliu et al., 2011). Thus, premature maturation together with membrane and cell wall disintegration seemed to be taking place simultaneously with increases in those compounds in BER fruit.

While impairment of cross-membrane transport increased intracellular concentration of organic acids and decreased import of hexose, cell wall synthesis impairment probably caused intracellular accumulation of disaccharide. Decreased membrane conductivity observed here reflected membrane channels impairment and the loss of membrane integrity and function previously speculated to occur in BER (Chen et al., 2001; Saure, 2001; Ho and White, 2005). In mammalian necrotic cell death glucose stabilizes membrane and delays its rupture and since necrotic cell death mechanism may have been conserved through eukaryotic kingdoms (Laporte et al., 2007), therefore, it can be assumed that reduced glucose import to BER fruit cells contributes membrane disintegration and rupture.

An interesting capability of the technique is the detection of phytohormones and phenols in single cells.

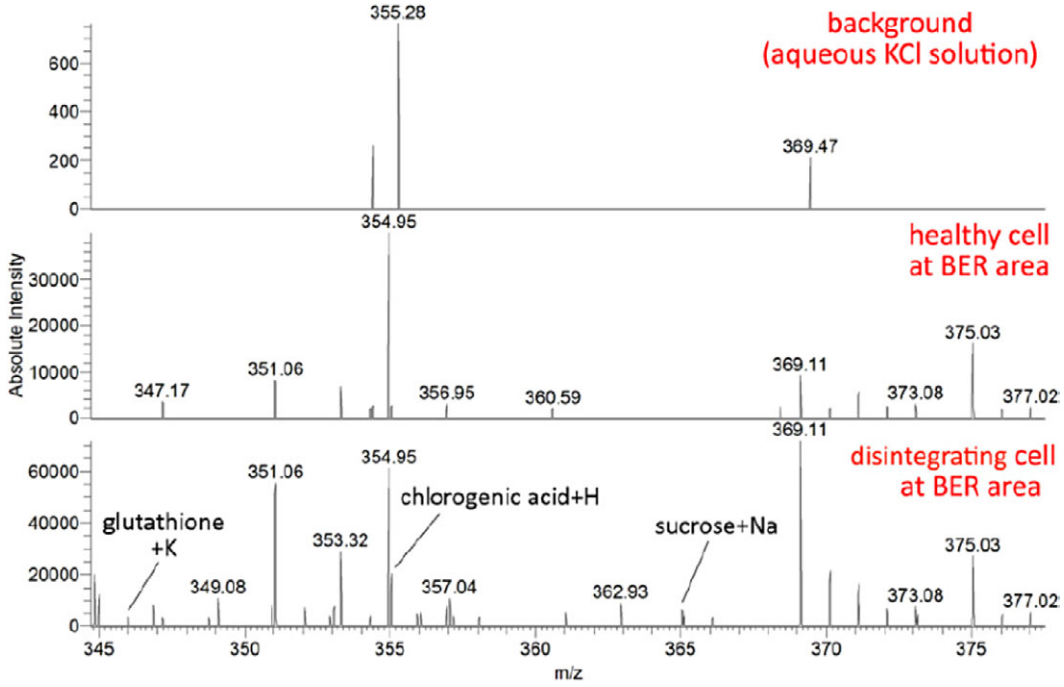

Fig. 8 PicoPPI mass spectra acquired by analyzing standard and cell solutions in positive ion mode; m/z 345–375.

Analyses of those metabolites led to the conclusion that precocious maturity and death processes activated before mechanical burst. The intracellular accumulation of ABA is a stress response and a possible signal for triggering precocious maturity-ripening process. Cell death processes are also related to salicylic acid (SA) (Dat et al., 2007), ascorbic acid (El-Shimi, 1993; Noctor and Foyer, 1998; Raven, 2000), and phenols (Buta and Spaulding, 1997; Dekock et al., 1980). SA biosynthesis activation occurs in plants exposed to biotic and abiotic stresses and involves in reactive oxygen species (ROS) production, and SA and ROS are considered as signals for triggering processes such as programmed cell death (Holuigue et al., 2007). On the other hand, ascorbic acid normally functions in scavenging ROS and controlling phenols and its decreased concentration along with increased SA directly influences the necrotic cell death process. It has been known that plant cell wall influences cell behavior and triggers cellular responses when plants encounter biotic stresses (Strauss, 1998). Since in BER fruits cell wall synthesis occurs abnormally, it is noteworthy to consider a possible role of cell wall in triggering cell death process, as well.

CONCLUSION

As outlined in the introduction we sought to establish a technique which is able to analyze both the water status and metabolites of single cells in real time within a few minute intervals. Prepared by the combination of two powerful techniques, the modular picoPPI Orbitrap MS is a tool for *in situ* probing and real time qualitative/quantitative analysis of living plant single cells. Consequently, while the technique facilitates plant metabolomics with single cell resolution, with concurrent water relations analyses it generates quantitative snapshot of the cell which can be used to explore growth or stress responses. We focused on BER-affected parenchyma cells whose bursting and necrotic death can be only explored at single cell level. The results of the analyses by picoPPI-MS showed that tissue breakdown and necrosis in blossom end rot primarily happens as the result of mechanical cell burst caused by hydrostatic pressure exerted on weakened cell wall. However, parallel precocious ripening and activated death processes contribute physiological degeneration of plasma membrane and cell wall. Abscisic acid was detected in damaged cells as a possible evidence of triggered precocious maturity. On the other hand, a sharp rise in the concentration of phenols and salicylic acid and decline in ascorbic acid reflected the activation of cell death process that would facilitate the deterioration of cell wall and plasma membrane.

ACKNOWLEDGEMENT

The authors are grateful for the financial support of a Grant-in-Aid (S) for H. N. (24228004) from the Japan Society for the Promotion of Science (JSPS) for Scientific Research. REB is a research member of CONICET (Argentina).

REFERENCES

Barros, J., Serrani-Yarce, J. C., Chen, F., Baxter, D., Venables, B. J., Dixon, R. A. 2016. Role of bifunctional ammonia-lyase in grass cell wall biosynthesis. Nat. Plants **2**: 16050.

Boyer, J. S. 1995. Measuring the Water Status of Plants and Soils (ed. by Boyer, J. S.), Chapter **4**: Pressure Probe, Academic Press, San Diego, p103–142.

Buta, J. G., Spaulding, D. W. 1997. Endogenous levels of phenolics in tomato fruit during growth and maturation. J. Plant Growth Regul. **16**: 43–46.

Carrari, F., Baxter, C., Usadel, B., Urbanczyk-Wochniak, E., Zanor, E.-I., Nunes-Nesi, A., Nikiforova, V., Centero, D.,

Ratzka, A., Pauly, M., Sweetlove, L. J., Fernie, A. R. 2006. Integrated analysis of metabolite and transcript levels reveals the metabolic shifts that underlie tomato fruit development and highlight regulatory aspects of metabolic network behavior. Plant Physiol. **142**: 1380–1396.

Chen, G. P., Wilson, I. D., Kim, S. H., Grierson, D. 2001. Inhibiting expression of a tomato ripening-associated membrane protein increases organic acids and reduces sugar levels of fruit. Planta **212**: 799–807.

Cohen, J. J. 1993. Apoptosis. Immunol Today **14**: 126–130.

Cooks, R. G., Ouyang, Z., Takats, Z., Wiseman, J. M. 2006. Ambient mass spectrometry. Science **311**: 1566–1570.

Dat, J. F., Capelli, N., Van Breusegem, F. 2007. The interplay between salicylic acid and reactive oxigen species during cell death in plants. In "Salicylic Acid A Plant Hormone" (ed. by Hayat, S., Ahmad, A.), Springer, Dordrecht, Netherlands, p 247–276.

DeBolt, S., Gutierrez, R., Ehrhardt, D. W., Melo, C. V., Ross, L., Cutler, S. R., Somerville, C., Bonetta, D. 2007. Morlin, an inhibitor of cortical microtubule dynamics and cellulose synthase movement. Proc. Natl. Acad. Sci. U.S.A. **104**: 5854–5859.

Dekock, P. C., Vaughan, D., Hall, A., Ord, B. G. 1980. Biochemical studies on blossom end rot of tomatoes. Physiol. Plant **48**: 312–316.

El-Shimi, N. M. 1993. Control of enzymatic browning in apple slices by using ascorbic acid under different conditions. Plant Foods Hum. Nutr. **43**: 71–76.

Fenn, J. B., Mann, M., Meng, C. K., Wong, S. F., Whitehouse, C. M. 1989. Electrospray ionization for mass spectrometry of large biomolecules. Science **246**: 64–71.

Gholipour, Y., Erra-Balsells, R., Hiraoka, K., Nonami, H. 2013. Living cell manipulation, manageable sampling, and shotgun picoliter electrospray mass spectrometry for profiling metabolites. Anal. Bioch. **433**: 70–78.

Gholipour, Y., Erra-Balsells, R., Nonami, H. 2012. *In situ* pressure probe sampling and UVMALDI MS for proling metabolites in living single cells. Mass Spectrom. **1**: A0003.

Gómez-Romero, M., Segura-Carretero, A., Fernández-Gutiérrez, A. 2010. Metabolite profiling and quantification of phenolic compounds in methanol extracts of tomato fruit. Phytochemistry **71**: 1848–1864.

Ho, L. C., White, P. J. 2005. A cellular hypothesis for the induction of blossom-end rot in tomato fruit. Ann. Bot. **95**: 571–581.

Holuigue, L., Salinas, P., Blanco, F., Garretón, V. 2007. Salicylic acid and reactive oxygen species in the activation of stress defence genes. In "Salicylic Acid A Plant Hormone" (ed. by Hayat, S., Ahmad, A.), Springer, Dordrecht, Netherlands, p 197–247.

Hossain, M. M., Nonami, H. 2011. Fruit growth of tomato associated with water uptake and cell expansion. J. Agric. Technol. **7**: 1049–1062.

Hossain, M. M., Nonami, H. 2012. Effect of salt stress on physiological response of tomato fruit grown in hydroponic culture system. Hortic. Sci. (Prague) **39**: 26–32.

http://solcyc.solgenomics.net (updated Oct. 2009) tomato metabolome database.

Hüsken, D., Steudle, E., Zimmermann, U. 1978. Pressure probe technique for measuring water relations of cells in higher plants. Plant Physiol. **61**: 158–163.

Jarvis, M. C. 1984. Structure and properties of pectin gels in plant cell walls. Plant Cell Environ. **7**: 153–227.

Laporte, C., Kosta, A., Klein, G., Aubry, L., Lam, D., Tresse, E., Luciani, M. F., Golstein, P. 2007. A necrotic cell death model in a protist. Cell Death Differ. **14**: 266–274.

Lyon, C. B., Beeson, K. C., Barrentine, M. 1942. Macro-element nutrition of the tomato plant as correlated with fruit fullness and occurrence of blossom-end rot. Bot. Gaz. **103**: 651–667.

Malone, M., Tomos, A. D. 1990. A simple pressure probe method for the dertermination of volume in higher plant cells. Planta **182**: 199–203.

Munoz-Espinoza, V. A., Lopez-Climent, M. F., Casaretto, J. A., Gomez-Cadenas, A. 2015. Water stress responses of tomato mutants impaired in hormone biosynthesis reveal abscisic acid, jasmonic acid and salicylic acid interactions. Front. Plant Sci. **6**: 997.

Moco, S., Bino, R. J., Vorst, O., Verhoeven, H. A., de Groot, J., van Beek, T. A., Vervoort, J., de Vos, C.H.R. 2006. A liquid chromatography-mass spectrometry-based metabolome database for tomato. Plant Physiol. **141**: 1205–1218.

Noctor, G., Foyer, C. 1998. Ascorbate and glutathion: keeping active oxygen under control. Annu. Rev. Plant Phys. Plant Mol. Biol. **49**: 249–279.

Nonami, H., Boyer, J. S. 1989. Turgor and growth at low water potentials. Plant Physiol. **89**: 798–804.

Nonami, H., Boyer, J. S. 1993. Direct demonstration of a growth-induced water potential gradient. Plant Physiol. **102**: 13–19.

Nonami, H., Fukuyama, T., Yamamoto, M., Yang, L., Hashimoto, Y. 1995. Blossom-end rot of tomato plants may not be directly caused by calcium deficiency. Acta Hortic. **396**: 107–114.

Nonami, H., Schulze, E.-D. 1989. Cell water potential, osmotic potential, and turgor in the epidermis and mesophyll of transpiring leaves. Planta **171**: 35–46.

Oms-Oliu, G., Hertog, M. L. A. T. M., Van de Poel, B., Ampofo-Asiama, J., Geeraerd, A. H., Nicolai, B. M. 2011. Metabolic characterization of tomato fruit during preharvest development, ripening, and postharvest shelf-life. Postharvest Biol. Technol. **62**: 7–16.

Pennell, R., Lamb, C. 1997. Programmed cell death in plants. Plant Cell **9**: 1157–1168.

Rajasekaran, L. R., Aspinall, D., Paleg, L. G. 2000. Physiological mechanism of tolerance of *Lycopersicon* spp. exposed to salt stress. Can. J. Plant Sci. **80**: 151–159.

Raven, E. L. 2000. Peroxidase-catalyzed oxidation of ascorbate. Structural, spectroscopic and mechanistic correlations in ascorbate peroxidase. Subcell Biochem. **35**: 317–349.

Saure, M. C. 2001. Blossom-end rot of tomato (*Lycopersicon esculentum* Mill.), a calcium- or a stress-related disorder? Sci. Hortic. **16**: 193–208.

Schauer, N., Zamir, D., Fernie, A. R. 2004. Metabolic profiling of leaves and fruit of wild species tomato: a survey of the *Solanum lycopersicum* complex. J. Exp. Bot. **56**: 297–307.

Shackel, K. A. 1987. Direct measurement of turgor and osmotic potential in individual epidermal cells. Plant Physiol. **83**: 719–722.

Strauss, E. 1998. When walls can talk, plant biologists listen. Science **282**: 28–29.

Taiz, L., Zeiger, E. 2006. Plant Physiology, 4th edition, Sinauer Associates, Inc., Sunderland, pp 700.

Tejedor, M. L., Mizuno, H., Tsuyama, N., Harada, T., Masujima, T. 2009. Direct sngle-cell molecular analysis of plant tissues by video mass spectrometry. Anal. Sci. **25**: 1053–1056.

Yildiz-Aktas, L., Dagnon, S., Gurel, A., Gesheva, E., Edreva, A. 2009. Drought tolerance in cotton: Involvement of non-enzymatic ROS-scavenging compounds. J. Agron. Crop Sci. **195**: 247–253.

Yu, Z., Chen, L. C., Suzuki, H., Ariyada, O., Erra-Balsells, R., Nonami, H., Hiraoka, K. 2009. Direct profiling of phytochemicals in tulip tissues and *in vivo* monitoring of the change of carbohydrate content in tulip bulbs by probe electrospray ionization mass spectrometry. J. Am. Soc. Mass Spectrom. **20**: 2304–2311.